Shaping Thiophene Oligomers into Fluorescent Nanobeads Forming Two-Dimensionally Patterned Assemblies by the Capillary Effect

M. Melucci,[†] C. Dionigi,[‡] G. Lanzani,[§] I. Viola,[⊥] G. Gigli,[⊥] and G. Barbarella[†]

Consiglio Nazionale Ricerche, Istituto per la Sintesi Organica e la Fotoreattività (ISOF), Via P. Gobetti 101, I-40129 Bologna, Italy; Consiglio Nazionale Ricerche, Istituto per lo Studio dei Materiali Nanostrutturati (ISMN), Via P. Gobetti 101, I-40129 Bologna, Italy; Dip. Fisica, Politecnico di Milano, P.za Leonardo da Vinci 32, I-20133 Milano, Italy; and National Nanotecnology Laboratory of CNR−INFM, Dip. Ingegneria Innovazione, Università di Lecce, Via Arnesano, I-73100 Lecce, Italy

Received July 22, 2005; Revised Manuscript Received September 13, 2005

ABSTRACT: We demonstrate that highly stable fluorescent nanobeads can be obtained by emulsion copolymerization of oligothiophene methyl methacrylates and styrene and that deposition on a planar surface by microfluidic lithography induces the spontaneous nanobead self-assembling. The average nanobead diameter was controlled in the submicron scale by varying the amount of surfactant used in the polymerization reaction. Photoluminescence and pump−probe experiments proved that the nanobeads had retained the optical signature of the oligothiophenes, yet preventing their aggregation. Scanning electron microscopy images of the self-assembled nanobeads are reported.

Introduction

The synthesis of nanosystems and their self-organization in ordered structures is a topic of great current concern in materials chemistry, and large multidisciplinary effort has been directed to the fabrication of nanometer-scale materials patterned in highly ordered two and three dimensions.[1]

Thiophene oligomers are chemically stable multifunctional molecular materials.[2] Changing the size, the nature of the substituents, or the substitution pattern allows for the tuning of their semiconductor, photonic and electroluminescence properties as well as their biological activity, for a great deal of applications in electrical and optical devices and in medical diagnostics.[3] Owing to their easy functionalization, different strategies can be designed to further improve their performance and applicability through the insertion of these molecules into more complex supramolecular structures and the creation of new functional nanostructures. In particular, the possibility to copolymerize thiophene oligomers with vinyl monomers—including styrene and methyl methacrylate, through emulsion, suspension, or dispersion processes[4]—offers the opportunity to generate nanoscale materials with a wealth of different tunable properties. Depending on the monomers and the chemical methodologies employed for polymerization, one could be able in principle to create nanometer-sized supramolecular structures characterized by the electrical and optical properties of the thiophene oligomers used as polymerization comonomers. As a part of a more extended investigation,[5] we sketch here a chemical strategy to shape thiophene oligomers into fluorescent nanobeads of controlled emission frequency and show that the nanobeads can be organized in ordered two-dimensional patterns by microfluidic lithography. We show that the microfluidic approach—a very versatile and low-cost procedure[6,7]—induces a regular pattern even in polydisperse beads that do not allow the spontaneous self-assembly into a regular hexagonal face-centered-cubic (fcc) lattice.

Results

I. Synthesis of Monomers and Nanobeads. The nanobeads were prepared by emulsion polymerization using terthiophenes **3** and **5** functionalized with the methyl methacrylate group at one terminal and one inner position, respectively, as the comonomers. The synthesis of **3** and **5**, starting from commercial 2-(2-hydroxyethyl)- and 3-(2-hydroxyethyl)thiophene, is shown in Scheme 1. Intermediates **1a**, **4a**, and **4b** have already been described.[8a] The synthesis of **2a** was achieved by taking advantage of microwave assistance.[8b] The methyl methacrylate group was introduced by using the general methodology employed for the esterification of carboxylic acids.[9]

Nanobead samples **B1**, **B2**, **BR1**, and **BR2** were prepared by emulsion polymerization of styrene and comonomers **3** and **5** running the reactions at 80 °C for 24 h, in the presence of a fluorinated anionic surfactant ($Cl(C_3F_6O)_2CF_2COO^-Na^+$, **6**) and using potassium persulfate as the free radical source. At the end of the polymerization reaction, the latexes were purified from the unreacted monomer and residual surfactant by repeated dialyses. In all the polymerization reactions, the amounts of styrene, fluorescent comonomers, and potassium persulfate as well as the water content were kept constant, whereas variations were allowed in the surfactant amount. The amount of surfactant employed in the preparation of samples **BR1** and **BR2** was 3 times that employed in the preparation of samples **B1** and **B2**. In all cases, stable latexes were obtained with nanobead yields ranging from 70 to 90% and nearly quantitative styrene conversions.

The zeta potential of the various samples was in the range −30 to −51 mV. Negative zeta potentials indicate that the latexes are stabilized by electrostatic repulsions of negative charges—from both the residual surfactant and the ionic initiator fragments—at the particles' sur-

[†] Istituto per la Sintesi Organica e la Fotoreattività (ISOF).
[‡] Istituto per lo Studio dei Materiali Nanostrutturati (ISMN).
[§] Politecnico di Milano.
[⊥] Università di Lecce.
* Corresponding author. E-mail: barbarella@isof.cnr.it.

10.1021/ma051602b CCC: $30.25
Published on Web 11/01/2005

Scheme 1. Synthesis of Methyl Methacrylates 3 and 5 and Copolymerization with Styrene[a]

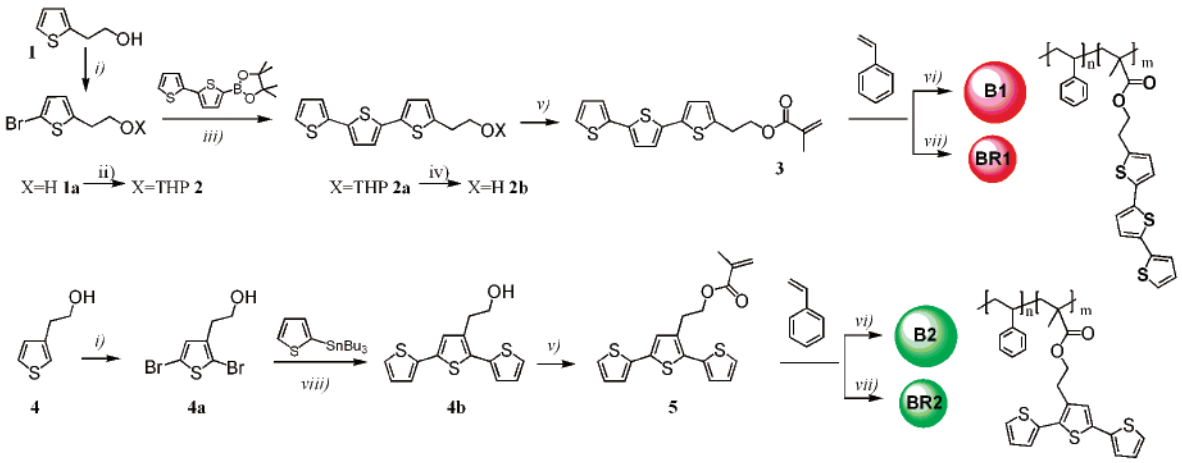

[a] (i) NBS, toluene, −20 °C;.(ii) 2-tetrahydropyranyl, CH_2Cl_2; (iii) KF/Al_2O_3−MeOH, $Pd(dppf)Cl_2$, MW 9′, 80 °C; (iv) HCl 10%,THF, reflux; (v) acryloyl acid, DCC, CH_2Cl_2; (vi) styrene, 80 °C, $Cl(C_3F_6O)_2CF_2COO^-Na^+$ (compound **6**, 1.65 mmol); (vii) styrene, 80 °C, $Cl(C_3F_6O)_2CF_2COO^-Na^+$ (6.6 mmol); (viii) 2-tributhylstannylthiophene, $Pd(AsPh_3)_4$, THF reflux.

Table 1. Amount of Fluorinated Anionic Surfactant and Characteristics of the Nanobeads Obtained in the Different Preparations

sample	surfactant **6**/ g (mmol)	fluorescent comonomer	av diam SEM/nm	zeta potential/mV
B1	0.8 (1.65)	**3**	470 ± 10	−30
B2	0.8 (1.65)	**5**	360 ± 10	−34
BR1	3.2 (6.60)	**3**	99 ± 10	−57
BR2	3.2 (6.60)	**5**	100 ± 10	−51

face. Samples **B1** and **B2** consist of polydisperse nanobeads with a mean size of 470 and 360 nm, whereas samples **BR1** and **BR2** are considerably smaller, with average sizes of 99 and 100 nm, respectively. Table 1 lists the amount of fluorinated anionic surfactant **6** for a given comonomer together with the diameter of the nanobeads obtained in the different preparations and the corresponding zeta potentials. The mean nanobead size was determined by scanning electron microscopy (SEM).

II. Photoluminescence Measurements. The photoluminescence spectra upon UV excitation of nanobeads **B1**, **BR1** and **B2**, **BR2** in suspension and cast film are reported in Figure 1.

The photoluminescence spectra in suspension correspond well to that of α-terthiophene (T3) in solution.[10] The emission bands display vibronic structures which are more or less accentuated depending on the nanobead size. Moreover, a slight red shift of the overall emission and an increase in the intensity of the low-energy peak, with respect to the high-energy one, are evident when the mean size of the nanobead is decreased (compare the spectra of sample **B1**(**B2**) with that of sample **BR1**(**BR2**)). A small variation of the emission energy is also observed in compounds with comparable nanobead size and the oligomer linked in a different position. In particular, sample **B1**(**BR1**) with the oligomer linked to the aliphatic chain via the terminal position shows a PL emission slightly red-shifted with respect to sample **B2** (**BR2**) with the oligomer linked via the internal ring. In cast films the emission bands are broader, but similar effects are observed.

Pump−probe experiments[11] were carried out only on cast films, since strong light scattering prevented the measurements to be carried out for the nanobeads in suspension. Figure 1c shows transient transmission difference traces for sample **BR2** at 610 and 460 nm after photoexcitation with 150 fs pulses at 390 nm.

The interpretation of these data is quite straightforward and consistent with the photophysical picture typical of oligothiophenes in solution.[10] At 610 nm we observed photoinduced absorption (PA), the measured decay of 155 ps being consistent with that reported in the literature for singlet state deactivation. At 460 nm we probe SE at the beginning, turning into PA due to singlet−triplet energy transfer and triplet−triplet absorption, as expected for this class of materials. The time constant observed and the lack of excitation density dependence suggests terthiophenes are isolated in the nanobead texture. Interestingly, we did observe a difference in the singlet state lifetime between **BR1** and **BR2** samples, the former being longer lived (about 210 ps). This might be caused by a different conformation of the oligomer.

III. Microfluidic-Induced Self-Assembly. Micromolding in capillaries is based on capillarity-induced filling of elastomeric channels by an appropriately diluted polymer.[6,7] In the present case elastomeric elements were obtained by silicon masters with 15 μm large stripes with a period of 30 μm and then treated by O_2 plasma to achieve hydrophilic surfaces (see the Experimental Section). Afterward, the replicas were wetted with an aqueous suspension of the nanobeads, which penetrated inside the elastomeric channels by the capillary effect.

The different bead order resulting at different microfluidic path lengths is noteworthy. The most ordered colloidal particles were deposited on a single layer on the top of the substrates and on the final regions of the filled capillaries, whereas a disordered packing was found on the deposited layers and at the entrance of the microchannels. The latter point can be explained by considering that the liquid dynamics at short time deviates from the Washburn-type power-law[12] for the liquid displacement, $z \approx t^{1/2}$, commonly used in the capillary approach. This deviation is usually ascribed to the variation of the contact line with the spreading velocity whose modification affects the molecules organization. Besides the different dynamics at the entrance of the channels, the different self-organization patterns indicate a sensible size selection effect inside the microfluidic channel. Such an effect can be ascribed to the

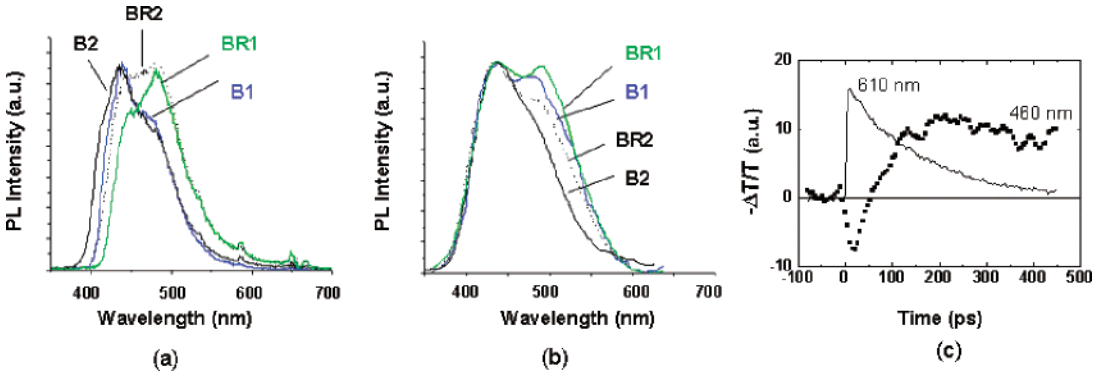

Figure 1. Photoluminescence spectra of nanobeads **B1**, **B2**, **BR1**, and **BR2** in suspension (a) and cast film (b) obtained upon excitation with a with a He−Cd laser (λ_{exc} 325 nm). (c) Transmission difference traces at 610 nm (PA) and 460 nm (SE/PA) in sample **BR2**, after photoexcitation at 390 nm with 150 fs pulses.

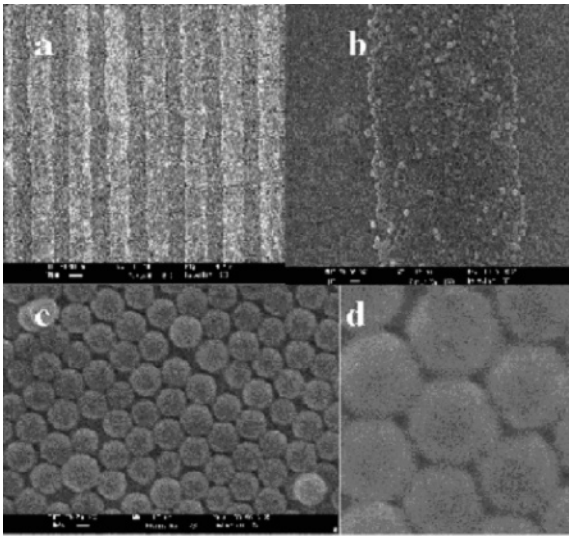

Figure 2. SEM micrographs of the microfluidic-induced self-assembly of nanobeads **B1**.

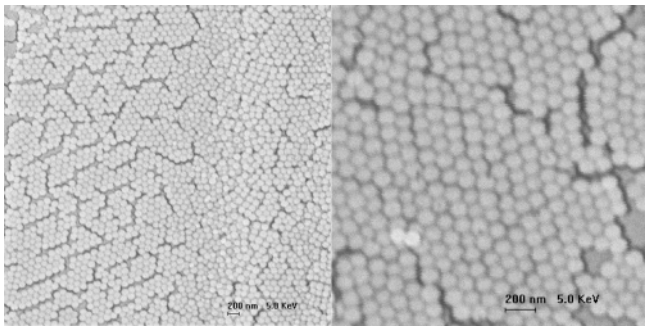

Figure 3. SEM micrographs of microfluidic-induced self-assembly of nanobeads **BR1**.

self- assembling tendency of equal-sized beads to segregate into a close-packing structure generating, in polydisperse beads**,** short-range ordered domains, as shown in Figures 2 and 3. The figures show self-assembled hexagonal small domains obtained by using an aqueous suspension of nanobeads with a diameter of 470 nm (**B1**) and 99 nm (**BR1**), respectively. It is seen from Figure 2a that the obtained striped pattern faithfully replicates the original master structure. Figure 2b displays a single stripe, in which areas are visible where the spheres are arranged according to an ordered hexagonal face-centered-cubic (fcc) structure. The colloidal particles are deposited on a single partially ordered layer (spheres deposited on the second (upper) layer can be appreciated in the image).

Figure 2c shows a higher resolution SEM picture where the hexagonal coordination can be noted. One can also see the defects introduced in the crystal because of the polydispersity of the colloidal particles. Figure 2d shows a magnified picture of the hexagonal structure formed by nanobeads **B1**.

Figure 3a,b shows that using the smaller spheres **BR1**, characterized by a smaller size dispersion, bigger ordered domains may be achieved. Such domains are principally marked by cracks along the grain boundaries, as generally observed also in opals fabricated by conventional vertical techniques.[13]

Discussion

Our data show that the functionalization of thiophene oligomers with the methacryloyl group and the copolymerization with styrene is a viable strategy to introduce thiophene oligomeric units into nonconjugated chains and to obtain stable fluorescent nanobeads with different mean size diameters by changing the amount of surfactant used in the polymerization process. The nanobead latexes are stable thanks to the residual surfactant and the ionic charges derived from the initiator residues. However, the presence of these ionic groups does not affect the fluorescence properties of the thiophene oligomers, as shown by the PL spectra and pump−probe experiments on the nanobeads in suspension, which shows that optical features and dynamics are very similar to those obtained for α-terthiophene in solution.[10] The time constant observed and the lack of excitation density dependence confirm that, in the conditions employed here, terthiophenes are "isolated" in the nanobead texture. Significant aggregation would have introduced new nonradiative states and decay paths, reducing the light emission, as it generally happens with unsubstituted oligothiophenes in the solid state, for which most optical applications—notably light emission and light amplification as in lasers—become impossible.[2] The relevance of the present approach is that it allows high molecular concentrations to be achieved without enhancing molecular interactions within nanostructures so that thiophene oligomers can mantain their intrinsic photonic properties. Of course, higher densities of the fluorophores will be investigated to set the limit one can reach before intermolecular quenching sets in.

No remarkable effects of the dimension of the nanobeads on fluorescence properties were found either. The

small shifts that can be observed in the spectra of Figure 1 from one type of nanobeads to the other are likely to come from small variations in the oligomer torsional angles and hence changes in the $\pi-\pi$ delocalization degree.

As shown in Figures 2 and 3, our fluorescent nanobeads, although polydisperse, self-organize by the capillary effect in short-range close-packing structures. They show different features according to the different correlation lengths, which depend on the modification of the displacement velocity along the microchannels. In wide regions of our samples, close-packed arrays of nanoparticles can be observed, originating crystalline domains separated by long cracks. It is evident that the defects in the crystalline structure are mainly due to the size distribution of the spheres, giving rise to some fluctuations in the lattice constant. Nevertheless, it should be considered that the cracks among crystalline domains, present in our microfluidics samples, may be ascribed to the strain induced by the shrinkage of the colloidal crystals during the drying process and are favored by the finite size of the template features.[13]

Concluding Remarks

The ability to control, at the nanoscale, molecular organization in space, molecular interactions, and supramolecular order is the critical issue for developing organic nanotechnology. Here we demonstrated the feasibility of the incorporation of functional thiophene oligomers onto polymeric nonconjugated chains to produce fluorescent nanobeads that can be patterned by microfluidic lithography. The approach is based on the concept of multifunctional materials with selective mission. Self-aggregation into nanobeads is embodied by styrene chains, while specific optical functions come from the attached chromophore, which can be chosen by purpose. This is a new and alternative approach to obtain nanostructured materials with optical functions by exploiting a simple, inexpensive technique, essentially based on self-assembly. Future developments can go far beyond this. Better control over nanobeads size dispersion can be achieved to aim at photonic bandgap systems with intrinsic "decoration" built in during the chemical synthesis. This suggests the use of proper chromophores in resonance with the characteristic scattering gap of the ordered structure, as a new approach toward light control and nanophotonics.

Experimental Section

Synthesis of Terthiophene Methyl Methacrylates. 2-(2-Hydroxyethyl)thiophene (**1**), 3-(2-hydroxyethyl)thiophene (**4**), *N*-bromosuccinimide, 1,4-dihydro-2*H*-pyran, acryloyl acid, *p*-toluensulfonic acid, Pd(dppf)Cl_2, and Al_2O_3 were commercial materials. Solvents were dried by standard procedures. The characterization of **1a**, **2a**, **2b**, **4a**, and **4b** has already been reported.[8a] Microwave-assisted procedures were based on previously reported methodologies.[8b]

5-Bromo-2-[(3-tetrahydropyranyloxy)ethyl]thiophene, **2**. To a solution of 2.450 g (0.018 mol) of (5-bromothiophen-2yl)ethanol in 15 mL of CH_2Cl_2 was added stepwise 1.19 g (0.014 mol) of 1,4-dihydro-2*H*-pyran and a catalytic amount of *p*-toluensulfonic acid, and the mixture was stirred overnight. Afterward the solution was first washed with K_2CO_3 (10%) and then with CH_2Cl_2; the organic phase was separated, dried over Na_2SO_4, and evaporated. The crude product was purified by silica gel chromathography using methylene chloride:ethyl acetate 70:30 v/v. A white oil was obtained. Yield 96%; MS (*m/z*) 291 [$M^{\bullet+}$]. ^{1}H ($CDCl_3$): δ 6.85 (d, 1H), 6.6 (d, 1H), 4.62 (t, 1H), 3.7 (m, 4H), 3.03 (m, 2H), 1.7 ppm (m, 6H).

5-[(3-Tetrahydropyranyloxy)ethyl]-2,2′:5′,2″-terthiophene, **2a**. A microwave oven reactor was charged with 374 mg (1.29 mmol) of compound **2** mixed with basic Al_2O_3. To make the mixture more homogeneous, 0.1−0.5 mL of methanol was added and evaporated under reduced pressure. Afterward 100 mg (0.12 mmol) of Pd(dppf)Cl_2 and 430 mg of KF followed by 413 mg (1.41 mmol) of 2-[2,2′]-bithienyl-5-yl(4,4,5,5-tetramethyl)-[1,3,2]dioxaborolane merged with 540 mg of KF dissolved in 2 mL of a saturated solution of KOH were added to the solid mixture. The mixture was first allowed to undergo the action of microwaves for 9 min at 80° C and then chromatographed using methylene chloride as the eluant. A light yellow viscous liquid was obtained (310 mg, yield 64%) whose characteristics corresponded to the desired product (**2a**, reported in ref 14a). Compound **2b**[8a] was obtained following treatment of **2a** with HCl.[8c]

5″-Methyl Methacrylate-2,2′:5′,2″-terthiophene, **3**. To a solution of 0.03 mL (0.31 mmol) of metacryloyl acid in 4 mL of CH_2Cl_2 was added 8 mg (0.06 mmol) of DMAP. Afterward 77 mg (0.37 mmol) of DCC was added, and the mixture was stirred for 15 min. Then 100 mg (0.34 mmol) of **2b** was added, and the mixture was stirred overnight. The mixture was filtered and washed first with a 4% solution of HCl and then with a solution of saturated $NaHCO_3$; the organic layer separated, dried over Na_2SO_4, and evaporated. The crude product was chromatographed using methylene chloride: pentane 80:20 v/v as the eluant. 88 mg of a light yellow solid was separated (72% yield). MS (*m/z*) 360 [$M^{\bullet+}$]. ^{1}H ($CDCl_3$): δ 7.21 (dd, 1H), 7.16 (dd, 1H), 7.06 (d, 1H), 7.01 (m, 3H), 6.78 (d, 1H), 6.16 (m, 1H), 5.6 (m, 1H), 4.38 (t, 2H), 3.18 (t, 2H), 1.97 ppm (s, 3H). ^{13}C ($CDCl_3$): 167.0, 139.4, 137.0, 136.1, 135.9, 135.73, 135.6, 127.7, 126.3, 125.8, 124.3, 124.1, 123.8, 123.5, 123.3, 64.7, 29.7, 18.5 ppm. IR (neat): 3421, 1710, 1167, 794, 696 cm^{-1}.

4′-Methyl Methacrylate-2,2′:5′,2″-terthiophene, **5**. To a solution of 0.01 mL (0.16 mmol) of metacryloyl acid in 2 mL of CH_2Cl_2 was added 4 mg (0.03 mmol) of DMAP. Afterward 39 mg (0.19 mmol) of DCC was added, and the mixture was stirred for 15 min. Then 50 mg (0.17 mmol) of **4b** was added, and the mixture was stirred overnight. The mixture was filtered and washed first with a 4% solution of HCl and then with a solution of saturated $NaHCO_3$; the organic layer separated, dried over Na_2SO_4, and evaporated. The crude product was chromatographed using methylene chloride: pentane 80:20 v/v as the eluant. 45 mg of a viscous oil was separated (74% yield). MS (*m/z*) 360 [$M^{\bullet+}$]. ^{1}H ($CDCl_3$): δ 7.34 (dd, 1H), 7.22 (dd, 1H), 7.16 (m, 2H), 7.08 (dd, 2H),7.07 (s, 1H), 7.01 (dd, 1H), 6.09 (m, 1H), 5.56 (m, 1H), 4.39 (t, 2H), 3.14 (t, 2H), 1.94 ppm (s, 3H). ^{13}C ($CDCl_3$): 167.1, 136.7, 136.0, 135.6, 134.96, 134.8, 131.0, 127.7, 127.5, 126.3, 126.3, 125.7, 125.6, 124.4, 123.6, 64.2, 28.6, 18.5 ppm. IR(neat): 3105, 2956, 1716, 1161, 794, 694 cm^{-1}.

Nanobeads Preparation and Characterization. Styrene (99%) was washed with 3 × 100 mL of 1.0 M sodium hydroxide, 3 × 100 mL of water, dried with anhydrous sodium sulfate, and stored at 5 °C. Potassium persulfate (98%) was used without further purification. Nanobead samples **B1**, **B2**, **BR1**, and **BR2** were prepared by emulsion polymerization of styrene in the presence of comonomers **3** and **5.** The emulsions were stabilized by a commercial fluorinated anionic surfactant having the structure $Cl(C_3F_6O)_2CF_2COO^-Na^+$ (**6**). In a typical emulsion polymerization, the appropriate amount of **6** was dissolved in 200 mL of water and placed in a three-neck round-bottom flask equipped with mechanical stirring (stirring speed 300 g/min), reflux condenser, and nitrogen inlet. The solution was heated to 80 °C under a nitrogen atmosphere, and then a solution of 25 mL (218 mmol) of styrene and 50 mg (139 μmol) of the relevant fluorescent comonomer was added. After 30 min, 70 mg of potassium persulfate, dissolved in 2.0 mL of water, was added to the mixture, and the reaction was allowed to proceed for 24 h. At the end of the reaction, the latex was cooled and purified by repeated dialysis against deionized water. The nanobead size was determined with a scanning electron microscope (SEM, Leica Stereoscan 440 and LION LVI istrumentation) and an accelerating voltage of 20 kV. The

samples were sputter-coated under vacuum with a thin layer (10−30 Å) of gold. The SEM photographs were digitalized, using the Kodak photo-CD system, and elaborated by the NIH Image (version 1.55, public domain) image processing program. From 100 to 150 individual microsphere diameters were measured for each sample. Electrophoretic mobility was measured with a Malvern Zetasizer 3000 HS. Each value is the average of five measurements. The instrument was checked using a latex with known zeta potential.

Photoluminescence measurements were performed on suspensions and thin films, cast from aqueous solution, by exciting the samples with a He−Cd laser (325 nm) and detecting the homogeneous signal by a CCD spectrograph.

Pump−probe experiments with 200 fs time resolution were carried out using a Ti:AlO_3 amplified laser system. Double-frequency pulses at 390 nm were used for excitation, while probe was provided by white light generation in a thin sapphire plate.

Microfluidic Lithography. The Si(1, 0, 0) substrates were hydroxylated by immersion in a piranha solution (3:1, H_2SO_4:H_2O_2) for 90 min, rinsed three times in deionized water for 5 min under ultrasonication at room temperature, and then dried by a flux of nitrogen. Poly(dimethylsiloxane) (PDMS) elastomeric elements were obtained by photolithographically made silicon masters with 15 μm large stripes and periodicity of 30 μm and then treated by O_2 plasma (3 s) (rf power = 50 W, dc bias = 340 V, pressure = 52 mTorr). In this way, we achieved hydrophilic surfaces favoring the capillary penetration of water inside the microchannels. Then the replicas were wetted by an aqueous solution of nanoparticles, which penetrated inside the elastomeric channels ($\cong$1 μm high) by the capillary effect a few minutes, and were removed after water evaporation. A few nanometers of gold was evaporated onto the patterned samples to favor the investigation by scanning electron microscopy.

Acknowledgment. This work was funded by projects Sistemi molecolari e supramolecolari complessi e biostrutturistica (CNR Agenzia2000) and Nanobiomolecular devices (FIRB RBNE01YSR8). Thanks are due to doctors Pierino Di Pietro and Katia Sparnacci for help with the synthesis of monomers and the polymerization reactions, respectively. Thanks are also due to Dr. Dario Pisignano for help with the microfluidics measurements.

References and Notes

(1) (a) Klabunde, K. J. *Nanoscale Materials in Chemistry*; Wiley-Interscience: New York, 2001. (b) Sayari, A.; Jaroniec, M. *Nanoporous Materials. Studies in Surface Science Catalysis*; Elsevier: Amsterdam, 2002. (c) Zhang, J. Z.; Liu, J.; Chen, S.; Liu, G. Y. *Self-Assembled Nanostructures*; Kluwer Academic/Plenum Publisher: New York, 2003. (d) Kuzmany, H.; Roth, S.; Fink, J. *Electronic Properties of Synthetic Nanostructures*: XVIII International Winterschool/Euroconference on Electronic Properties of Novel Materials, AIP Conference Proceedings 2004, No. 723.

(2) (a) Fichou, D. *Handbook of Oligo and Polythiophenes*; Wiley-VCH: New York, 1999. (b) Müllen, K.; Wegner, G. *Electronic Materials: The Oligomer Approach*; Wiley-VCH: New York, 1998. (c) Nalwa, H. S. *Handbook of Organic Conductive Molecules and Polymers;* J. Wiley & Sons: Chichester, 1997.

(3) Barbarella, G.; Melucci, M.; Sotgiu, G. *Adv. Mater.* **2005**, *17*, 1581.

(4) (a) Imae, I.; Nawa, K.; Ohsedo, Y.; Noma, N.; Shirota, Y. *Macromolecules* **1997**, *30*, 380. (b) Ohsedo, Y.; Imae, I.; Shirota, Y. *J. Polym. Sci., Part B* **2003**, *41*, 2471. (c) Giani, E.; Sparnacci, K.; Laus, M. *Macromolecules* **2003**, *36*, 4360. (d) Sparnacci, K.; Laus, M.; Tondelli, L.; Magnani, L.; Bernardi, C. *Macromol. Chem. Phys.* **2002**, *203*, 1364. (e) Caputo, A.; Betti, M.; Altavilla, G.; Bonaccorsi, G.; Boarini, C.; Marchisio, M.; Butto, S.; Sparnacci, K.; Laus, M.; Tondelli, L.; Ensoli, B. *Vaccine* **2002**, *20*, 2303. (f) Sparnacci, K.; Laus, M.; Lelli, M.; Vannini, R.; Tondelli, L. *J. Polym. Sci., Polym. Chem.* **2000**, *38*, 3347.

(5) Melucci, M.; Barbarella, G.; Zambianchi, M.; Benzi, M.; Biscarini, F.; Cavallini, M.; Bongini, A.; Fabbroni, S.; Mazzeo, M.; Anni, M.; Gigli, G. *Macromolecules* **2004**, *37*, 5692.

(6) (a) McDonad, J. C.; Whitesides, G. M. *Acc. Chem. Res.* **2002**, *35*, 491. (b) Kim, E.; Xia, Y.; Whitesides, G. M. *J. Am. Chem. Soc.* **1996**, *118*, 5722. (c) Kim, E.; Xia, Y.; Whitesides, G. M. *Chem. Mater.* **1996**, *8*, 1558.

(7) Pisignano, D.; Sariconi, E.; Mazzeo, M.; Gigli, G.; Cingolani, R. *Adv. Mater.* **2002**, *14*, 1565.

(8) (a) Barbarella, G.; Zambianchi, M.; Pudova, O.; Paladini, V.; Ventola, A.; Cipriani, F.; Gigli, G.; Cingolani, R.; Citro, G. *J. Am. Chem. Soc.* **2001**, *123*, 11600. (b) Melucci, M.; Barbarella, Sotgiu, G. *J. Org. Chem.* **2002**, *67*, 8877. (c) Barbarella, G.; Zambianchi, M.; Bongini, A.; Antolini, L. *J. Org. Chem.* **1996**, *61*, 4708.

(9) Neises, B.; Steglich, W. *Angew. Chem., Int. Ed. Engl.* **1978**, *17*, 522.

(10) (a) Lanzani, G.; Cerullo, W.; Stagira, S.; De Silvestri, S.; Garnier, F. *J. Chem. Phys.* **1999**, *111*, 6474. (b) Oelkrug, D.; Egelhaaf, H. J.; Gierschner, J.; Tompert, A. *Synth. Met.* **1996**, *76*, 249. (c) Kanemitsu, Y.; Suzuki, K.; Masumoto, Y.; Tomiuchi, Y.; Shiraishi, Y.; Kuroda, M. *Phys. Rev. B* **1994**, *50*, 2301.

(11) Comoretto, D.; Lanzani, G. In *Organic Photovoltaics;* Brabec, C. J., Dyakonov, V., Parisi, J., Sariciftci, N. S., Eds.; Springer-Verlag: Berlin, 2003; pp 57−84.

(12) Darhuber, A.; Troian, S. M. *Phys. Rev. E* **2001**, *64*, 031603.

(13) Ferrand, P.; Minty, M. J.; Egen, M.; Ahopelto, J.; Zentel, R.; Romanov, S. G.; Sotomayor Torres, C. M. *Nanotechnology* **2003**, *14*, 323.

MA051602B